

Theoretical formulations on thermodynamics of quantum impurity systems

Hong Gong,* Yao Wang,* Hou-Dao Zhang, Rui-Xue Xu, Xiao Zheng, and YiJing Yan†
Hefei National Laboratory for Physical Sciences at the Microscale and Synergetic Innovation
Center of Quantum Information and Quantum Physics and Collaborative Innovation
Center of Chemistry for Energy Materials (iChEM) and Department of Chemical Physics,
University of Science and Technology of China, Hefei, Anhui 230026, China

(Dated: August 19, 2020; Submit to PRB)

In this work, we put forward the theoretical foundation toward thermodynamics of quantum impurity systems measurable in experiments. The theoretical developments involve the identifications on two types of thermodynamic entanglement free-energy spectral functions for impurity systems that can be either fermionic or bosonic or combined. Consider further the thermodynamic limit in which the hybrid environments satisfy the Gaussian–Wick’s theorem. We then relate the thermodynamic spectral functions to the local quantum impurity systems spectral densities that are often experimentally measurable. Another type of inputs is the bare–bath coupling spectral densities, which could be accurately determined with various methods. Similar relation is also established for the nonentanglement component that exists only in anharmonic bosonic impurity systems. For illustration, we consider the simplest noninteracting systems, with focus on the strikingly different characteristics between the bosonic and fermionic scenarios.

PACS numbers: 05.70.-a, 05.30.-d

I. INTRODUCTION

Quantum impurity systems such as quantum dots and nanostructured materials offer diversified functionalities, where the strong correlations, quantum entanglement, coherence and decoherence often play crucial roles. The properties such as electronic and heat conductivity of nano-materials can be enhanced significantly compared to their bulk counterparts.^{1–3} These unique properties can be exploited to design highly efficient molecular junctions and quantum devices.^{4–8} All these frontier developments need to be guided by basic thermodynamic principles in the quantum regime.⁹ The ever increasing capability in the exquisite manipulations and detections leads to quantum impurity systems also ideal test beds for quantum physics. However, can thermodynamics be experimentally measurable, particularly for quantum impurity systems? This is an open question to be addressed.

In this paper, we will exploit some basic relations toward the above quest. As Einstein remarked, “*Thermodynamics is the only physical theory which I am convinced will never be overthrown, within the framework of applicability of its basic concepts*”.¹⁰ On this basis, we elucidate a set of universal relations between mesoscopic quantum mechanics and macroscopic thermodynamics.

Physically, one can visualize a quantum impurity system as a thermodynamic mixture, such as the widely used Anderson impurity model. The total system–and–bath composite Hamiltonian assumes the form of $H_T = H_S + h_B + H_{SB}$. The last term denotes the hybridization between the local mesoscopic system and a nonlocal macroscopic bath environment. In the thermodynamics nomenclature, such a total composite mixture at a given temperature T constitutes a closed system. It is in thermal contact with surrounding heat reservoir to maintain the constant temperature scenario.

We will see in Sec. II there is a difference between the fermionic and bosonic hybridization scenarios. The former has only the entanglement component, but the latter involves also the nonentanglement contribution. Both these two thermodynamic components could be experimentally measured.

In Sec. III, we present a unified theory and relate the entanglement thermodynamics to two types of spectral functions. One is the entanglement free–energy spectral density, with odd parity in frequency. Another is the entanglement thermodynamic spectrum, with even parity in frequency. Interestingly, these two spectral functions possess opposite parity, but equal–area in the half–side frequency region of $\omega \in [0, \infty)$. While both are about equally accessible in experiments, we would suggest the thermodynamic spectrum be the choice. In Appendix, we analyze the universal high–temperature thermodynamic behaviors. We show the dramatic difference between the fermionic and bosonic hybridization scenarios.

Consider further the theoretical formulations with Gaussian bath environments, where the Gaussian–Wick’s theorem is applicable.^{11–13} This coupling bath model is rather commonly adopted in various theories in quantum mechanics of open systems, such as the path–integral influential functional formalism.^{14–16} Its time–derivative equivalence, the hierarchical equations of motion (HEOM) formalism, either bosonic^{17–20} or fermionic,²¹ is now a well–established method.^{22–29} The dissipaton equation of motion theory is also developed.^{30–33} This is a statistical quasi–particle extension of the HEOM, covering further the hybrid bath dynamics.^{30–35}

We will show that the system–and–bath entanglement theory with Gaussian environments³⁶ is intimately related to the aforementioned entanglement free–energy spectral functions. We will further extend this theory to its treatment on the nonentanglement thermodynamic

component that is generally nonzero for bosonic quantum impurity systems. We present the formulations with fermionic and bosonic Gaussian environments in Sec. IV and Sec. V, respectively. We conclude that the thermodynamic hybridizing free-energy, either fermionic or bosonic, can be completely determined with the *local impurity system* properties and the nonlocal bath hybridization functions. These two types of properties of quantum impurity systems are in principle both experimentally measurable. In Sec. VI, we illustrate the results on noninteracting systems and show the remarkably distinct bosonic versus fermionic characteristics. We summarize this paper with Sec. VII.

II. ENTANGLEMENT VERSUS NONENTANGLEMENT THERMODYNAMICS

A. Thermodynamic integral formalism

We will focus on the free-energy change before and after hybridization:

$$A_{\text{hyb}}(T) \equiv A(T) - A_0(T). \quad (2.1)$$

This corresponds to $Z_{\text{hyb}} = e^{-\beta A_{\text{hyb}}} = Z_{\text{T}}/Z_0$, with $\beta = 1/(k_B T)$, whereas $Z_{\text{T}} = e^{-\beta A} = \text{Tr} e^{-\beta H_{\text{T}}}$ and $Z_0 = e^{-\beta A_0} = Z_0^{\text{S}} Z_0^{\text{B}} = (\text{tr}_{\text{S}} e^{-\beta H_{\text{S}}})(\text{tr}_{\text{B}} e^{-\beta h_{\text{B}}})$. One can evaluate $Z_{\text{hyb}} = e^{-\beta A_{\text{hyb}}}$ directly via the imaginary-time approaches, such as the path-integral formalism³⁷ and its influential functional derivative equivalence.^{38–40}

Alternatively, according to the Second Law, one can relate the isotherm free-energy change to the *reversible work* performed on total composite mixture. This results in $A_{\text{hyb}}(T)$ the thermodynamic integral formalism, with the varying system–bath coupling strength as the integration parameter.^{41–44} To proceed, we write the total composite Hamiltonian in the hybridization parameter λ -augmented form,

$$H_{\text{T}}(\lambda) = H_{\text{S}} + h_{\text{B}} + \lambda H_{\text{SB}}. \quad (2.2)$$

A reversible process is now mathematically described with the smooth varying the hybridization parameter from $\lambda = 0$ to $\lambda = 1$. Denote $\hat{\rho}_{\text{T}}^{\text{eq}}(T; \lambda) \equiv e^{-\beta H_{\text{T}}(\lambda)}/Z_{\text{T}}(\lambda)$. The *differential reversible work* performed in $[\lambda, \lambda + d\lambda]$ is then

$$\delta w_{\text{rev}}(\lambda) = \text{Tr}[H_{\text{SB}} \hat{\rho}_{\text{T}}^{\text{eq}}(T; \lambda)] d\lambda. \quad (2.3)$$

We obtain the thermodynamic integral expression,^{41–44}

$$A_{\text{hyb}}(T) = \int_0^1 \delta w_{\text{rev}}(\lambda) = \int_0^1 \frac{d\lambda}{\lambda} \langle H_{\text{SB}} \rangle_{\lambda}, \quad (2.4)$$

with

$$\langle H_{\text{SB}} \rangle_{\lambda} \equiv \text{Tr}[(\lambda H_{\text{SB}}) \hat{\rho}_{\text{T}}^{\text{eq}}(T; \lambda)]. \quad (2.5)$$

This is just the λ -augmented equivalence to the original $\langle H_{\text{SB}} \rangle$ where $\lambda = 1$. Therefore, all methods on $\langle H_{\text{SB}} \rangle$

would be readily applicable for thermodynamics. These include the quantum Monte Carlo approach,^{45,46} density matrix renormalization group,^{47,48} numerical renormalization group,^{49,50} Green's function technique⁵¹ and multi-configuration time-dependent Hartree method.^{52,53} It is also noticed that the above formalism, Eq. (2.4) with Eq. (2.5), can be readily generalized to transient thermodynamics problems.⁵⁴

B. Entangled and nonentangled contributions

In general the system–bath coupling H_{SB} assumes a multiple-modes decomposition form, with each mode being a product of a system operator and a bath operator. The hybridization pair of operators can be either bosonic or fermionic. The resultant $\langle H_{\text{SB}} \rangle$ differs in these two scenarios, as detailed below.

1. Bosonic hybridization case

The generic form of bosonic hybridization reads

$$H_{\text{SB}} = \sum_u \hat{Q}_u \hat{F}_u, \quad \text{with } [\hat{Q}_u, \hat{F}_v] = 0. \quad (2.6)$$

Here, $\{\hat{Q}_u\}$ and $\{\hat{F}_u\}$ are Hermitian operators in the local impurity system and the nonlocal bath subspaces, respectively. Let $\delta \hat{O} \equiv \hat{O} - \langle \hat{O} \rangle$. We have

$$\langle H_{\text{SB}} \rangle = \sum_u \langle \hat{Q}_u \rangle \langle \hat{F}_u \rangle + \sum_u \langle \delta \hat{Q}_u \delta \hat{F}_u \rangle. \quad (2.7)$$

It involves both the uncorrelated and the nonlocally correlated sum terms. Their λ -augmented counterparts give rise the nonentanglement and entanglement free-energy contributions to Eq. (2.4), respectively. The former reads

$$A_{\text{hyb}}^{\text{nen}}(T) = \sum_u \int_0^1 \frac{d\lambda}{\lambda} \langle \hat{Q}_u \rangle_{\lambda} \langle \hat{F}_u \rangle_{\lambda}, \quad (2.8)$$

where

$$\begin{aligned} \langle \hat{Q}_u \rangle_{\lambda} &= \text{Tr}[\hat{Q}_u \hat{\rho}_{\text{T}}^{\text{eq}}(T; \lambda)], \\ \langle \hat{F}_u \rangle_{\lambda} &= \text{Tr}[\lambda \hat{F}_u \hat{\rho}_{\text{T}}^{\text{eq}}(T; \lambda)]. \end{aligned} \quad (2.9)$$

Similarly, the entanglement free-energy contribution is

$$A_{\text{hyb}}^{\text{en}} \equiv A_{\text{hyb}} - A_{\text{hyb}}^{\text{nen}} = \sum_u \int_0^1 \frac{d\lambda}{\lambda} \langle \delta \hat{Q}_u \delta \hat{F}_u \rangle_{\lambda}. \quad (2.10)$$

2. Fermionic hybridization case

In contrast to Eq. (2.6), a fermionic hybridization usually reads

$$H_{\text{SB}} = \sum_u (\hat{a}_u^{\dagger} \hat{F}_u + \hat{F}_u^{\dagger} \hat{a}_u), \quad \text{with } \{\hat{a}_u^{\dagger}, \hat{F}_v\} = 0. \quad (2.11)$$

Here, $\{\hat{a}_u\}$ and $\{\hat{F}_u\}$ are fermionic operators in the local impurity system and the nonlocal bath subspaces, respectively, satisfying $\{\hat{a}_u^\dagger, \hat{F}_v\} = \{\hat{a}_u, \hat{F}_v\} = 0$. In practice, \hat{a}_u (\hat{a}_u^\dagger) is the annihilation (creation) operator, associated with the specified single-electron spin-orbital state in the system subspace. The nonlocal bath subspace operator \hat{F}_u consists of a linear combination annihilation operators in the bath subspace. Apparently, $\langle \hat{a}_u^\dagger \rangle = \langle \hat{F}_u \rangle = 0$, due to the underlying fermionic nature. Therefore, the fermionic hybridization is a pure entanglement event, with

$$A_{\text{hyb}} = A_{\text{hyb}}^{\text{en}} = \sum_u \int_0^1 \frac{d\lambda}{\lambda} \langle \hat{a}_u^\dagger \hat{F}_u + \hat{F}_u^\dagger \hat{a}_u \rangle_\lambda. \quad (2.12)$$

In the coming section, we will focus on the entanglement thermodynamics via Eq. (2.10) and Eq. (2.12) for the bosonic and fermionic scenarios, respectively. We will identify the spectral density descriptions on entanglement thermodynamics that is intimately related to the fluctuation-dissipation theorem (FDT).^{11–13} The nonentanglement $A_{\text{hyb}}^{\text{nen}}$, Eq. (2.8), which exists only for the bosonic case, will be revisited in Sec. V.

III. ENTANGLEMENT THERMODYNAMIC SPECTRAL FUNCTIONS

A. Entanglement spectral density: Bosonic case

It is noticed that the entanglement thermodynamics can be treated with the linear response theory, without approximations. In the following developments, we set the time variable $t \geq 0$, unless specified further. Consider the bosonic case, Eq. (2.6), where $[\hat{Q}_u, \hat{F}_u] = 0$. The relevant response function with the *system-and-bath symmetrization* would be

$$\chi_{\text{SB}}(t) = \frac{i}{2} \sum_u \langle [\hat{Q}_u(t), \hat{F}_u(0)] + [\hat{F}_u(t), \hat{Q}_u(0)] \rangle. \quad (3.1)$$

This is a real and odd function. Define

$$\tilde{\chi}_{\text{SB}}(\omega) \equiv \int_0^\infty dt e^{i\omega t} \chi_{\text{SB}}(t) \equiv \tilde{\chi}_{\text{SB}}^{(r)}(\omega) + i\tilde{\chi}_{\text{SB}}^{(i)}(\omega). \quad (3.2)$$

The real and imaginary parts, $\tilde{\chi}_{\text{SB}}^{(r)}(\omega) \equiv \text{Re}\tilde{\chi}_{\text{SB}}(\omega)$ and $\tilde{\chi}_{\text{SB}}^{(i)}(\omega) \equiv \text{Im}\tilde{\chi}_{\text{SB}}(\omega)$, satisfy $\tilde{\chi}_{\text{SB}}^{(r)}(-\omega) = \tilde{\chi}_{\text{SB}}^{(r)}(\omega)$ and $\tilde{\chi}_{\text{SB}}^{(i)}(-\omega) = -\tilde{\chi}_{\text{SB}}^{(i)}(\omega)$, respectively. The related spectral density is given by

$$\mathcal{J}_{\text{SB}}(\omega) \equiv \frac{1}{2i} \int_{-\infty}^\infty dt e^{i\omega t} \chi_{\text{SB}}(t) = \text{Im}\tilde{\chi}_{\text{SB}}(\omega). \quad (3.3)$$

Throughout this paper, we set $\hbar = 1$ for the unit of Planck constant. Denote also $\hat{O}(t) \equiv e^{iH_{\text{T}}t} \hat{O} e^{-iH_{\text{T}}t}$ and $\langle\langle \cdot \rangle\rangle \equiv \text{Tr}_{\text{T}}[(\cdot) e^{-\beta H_{\text{T}}}] / Z_{\text{T}}$, with $H_{\text{T}} \equiv H_{\text{T}}(\lambda = 1)$. This defines $\chi_{\text{SB}}(t)$ of Eq. (3.1). Its λ -augmented counterpart,

$\chi_{\text{SB}}(t; \lambda)$, is similar but with $H_{\text{T}}(\lambda)$ of Eq. (2.2). The resultant $\tilde{\chi}_{\text{SB}}(\omega; \lambda)$ and $\mathcal{J}_{\text{SB}}(\omega; \lambda)$ are followed as Eqs. (3.2) and (3.3). The above convention follows that in Sec. II and is adopted throughout this paper.

To evaluate Eq. (2.10), we exploit the following identity that arises from the bosonic FDT,

$$\langle H_{\text{SB}} \rangle_\lambda^{\text{en}} = \sum_u \langle \delta \hat{Q}_u \delta \hat{F}_u \rangle_\lambda = \frac{1}{\pi} \int_{-\infty}^\infty d\omega \frac{\mathcal{J}_{\text{SB}}(\omega; \lambda)}{1 - e^{-\beta\omega}}. \quad (3.4)$$

One can then recast Eq. (2.10) as

$$A_{\text{hyb}}^{\text{en}}(T) = -\frac{1}{\pi} \int_{-\infty}^\infty d\omega \frac{\varphi(\omega)}{1 - e^{-\beta\omega}}, \quad (3.5)$$

with the entanglement free-energy spectral density,

$$\varphi(\omega) \equiv -\text{Im} \int_0^1 \frac{d\lambda}{\lambda} \tilde{\chi}_{\text{SB}}(\omega; \lambda) = -\varphi(-\omega). \quad (3.6)$$

The inclusion of a negative sign to each of Eqs. (3.5) and (3.6) is made with the spontaneity convention. The last identity highlights that the entanglement free-energy spectral density, $\varphi(\omega)$, is *antisymmetric*. This symmetry is rooted at the chosen *system-and-bath symmetrization* response function, Eq. (3.1). It turns out to be instrumental to the entanglement thermodynamic spectrum, as detained in Sec. III C.

B. Entanglement spectral density: Fermionic case

It is noticed that convention theories of fermionic impurity systems go with the Green's function formalism, involving anticommutators between two non-Hermitian operators. In relation to the evaluation of

$$\langle H_{\text{SB}} \rangle = \sum_u \langle \hat{a}_u \hat{F}_u^\dagger + \hat{F}_u \hat{a}_u^\dagger \rangle, \quad (3.7)$$

the relevant Green's function is

$$G_{\text{SB}}(t) = \sum_u \langle \{ \hat{a}_u(t), \hat{F}_u^\dagger(0) \} + \{ \hat{F}_u(t), \hat{a}_u^\dagger(0) \} \rangle. \quad (3.8)$$

It satisfies

$$G_{\text{SB}}^*(t) = G_{\text{SB}}(-t) \quad \text{and} \quad G_{\text{SB}}(0) = 0. \quad (3.9)$$

Define [cf. Eq. (3.2)]

$$\tilde{G}_{\text{SB}}(\omega) \equiv \int_0^\infty dt e^{i\omega t} G_{\text{SB}}(t). \quad (3.10)$$

The related spectral density is given by

$$\mathcal{J}_{\text{SB}}(\omega) = \frac{1}{2} \int_{-\infty}^\infty dt e^{i\omega t} G_{\text{SB}}(t) = \text{Re} \tilde{G}_{\text{SB}}(\omega), \quad (3.11)$$

satisfying

$$\int_{-\infty}^\infty d\omega \mathcal{J}_{\text{SB}}(\omega) = \pi G_{\text{SB}}(t=0) = 0. \quad (3.12)$$

We obtain

$$\langle H_{\text{SB}} \rangle = \frac{1}{\pi} \int_{-\infty}^{\infty} d\omega \frac{\mathcal{J}_{\text{SB}}(\omega)}{1 + e^{\beta\omega}} = \frac{1}{\pi} \int_{-\infty}^{\infty} d\omega \frac{\mathcal{J}_{\text{SB}}^{\text{odd}}(\omega)}{1 + e^{\beta\omega}}. \quad (3.13)$$

The first identity arises from the fermionic FDT. The last one is the integrated equality, in which $\mathcal{J}_{\text{SB}}(\omega)$ can be replaced by its odd function component,

$$\mathcal{J}_{\text{SB}}^{\text{odd}}(\omega) \equiv \frac{1}{2} [\mathcal{J}_{\text{SB}}(\omega) - \mathcal{J}_{\text{SB}}(-\omega)] = -\mathcal{J}_{\text{SB}}^{\text{odd}}(-\omega). \quad (3.14)$$

The observations are as follows. Consider the symmetry property of Fermi function,

$$\frac{1}{1 + e^{\beta\omega}} = \frac{1}{2} - \frac{\sinh(\beta\omega/2)}{2 \cosh(\beta\omega/2)}. \quad (3.15)$$

The first term, the constant (1/2), does not contribute to Eq. (3.13), due to Eq. (3.12). The second term is an odd function, resulting in the integrated equality, the second identity of Eq. (3.13).

Now it is readily to obtain Eq. (2.12) the expression,

$$A_{\text{hyb}}(T) = A_{\text{hyb}}^{\text{en}}(T) = -\frac{1}{\pi} \int_{-\infty}^{\infty} d\omega \frac{\varphi(\omega)}{1 + e^{\beta\omega}}. \quad (3.16)$$

The involved free-energy spectral density reads

$$\varphi(\omega) = -\frac{1}{2} \text{Re} \int_0^1 \frac{d\lambda}{\lambda} \left[\tilde{G}_{\text{SB}}(\omega; \lambda) - \tilde{G}_{\text{SB}}(-\omega; \lambda) \right], \quad (3.17)$$

with $\varphi(-\omega) = -\varphi(\omega)$, the same parity as Eq. (3.6).

C. Entanglement free-energy spectrum and the equal-area theorem

Following Eq. (3.2) and Eq. (3.10), we have

$$\tilde{\chi}_{\text{SB}}(z; \lambda) \equiv \int_0^{\infty} dt e^{izt} \chi_{\text{SB}}(t; \lambda), \quad (3.18)$$

$$\tilde{G}_{\text{SB}}(z; \lambda) \equiv \int_0^{\infty} dt e^{izt} G_{\text{SB}}(t; \lambda). \quad (3.19)$$

These are analytical functions of z in the upper-half plane. It is noticed that the fermionic $\varphi(\omega)$, Eq. (3.17), engages both $\tilde{G}_{\text{SB}}(z; \lambda)$ and $\tilde{G}_{\text{SB}}(-z; \lambda)$. The latter is an analytical functions of z in the lower-half plane. Apparently, the above specified nature of analytical functions preserves in their λ -integrals. We can then perform the frequency integration in both Eq. (3.5) and Eq. (3.16), by using the Cauchy's contour integration technique. The poles inside the individual half-plane contour integration arise only from the Matsubara frequencies.

The Cauchy's contour integration evaluations on Eq. (3.5) and Eq. (3.16) result in the unified expression,

$$A_{\text{hyb}}^{\text{en}}(T) = -\frac{\delta^{\pm}}{\beta} \vartheta(0) \pm \frac{2}{\beta} \sum_{n=1}^{\infty} \vartheta(\varpi_n^{\pm}). \quad (3.20)$$

Here, $\delta^+ = 0$ and $\delta^- = 1$ for the fermionic and bosonic cases, respectively. The second term engages the Matsubara frequencies, $\{\varpi_n^{\pm} = (2n - 1 + \delta^{\pm})\pi/\beta; n = 1, \dots, \infty\}$.

Two remarkable implications arises from Eq. (3.20). Firstly, it defines the so-called entanglement free-energy spectrum, $\vartheta(\varpi)$, as follows. By comparing between the bosonic Eq. (3.20) and Eq. (3.5) with Eq. (3.6), we obtain

$$\vartheta(\varpi \geq 0) = -\int_0^1 \frac{d\lambda}{\lambda} \tilde{\chi}_{\text{SB}}(i\varpi; \lambda) = \vartheta^*(\varpi). \quad (3.21)$$

Its fermionic counterpart can be identified by comparing between the fermionic Eq. (3.20) and Eq. (3.16) with Eq. (3.17). It results in

$$\vartheta(\varpi \geq 0) = \text{Im} \int_0^1 \frac{d\lambda}{\lambda} \tilde{G}_{\text{SB}}(i\varpi; \lambda). \quad (3.22)$$

In fact, $\tilde{\chi}_{\text{SB}}(i\varpi; \lambda)$ and $\tilde{G}_{\text{SB}}(i\varpi; \lambda)$ via Eqs. (3.18) and (3.19) are the Laplace transformations, with $s = \varpi$, on $\chi_{\text{SB}}(t; \lambda)$ and $G_{\text{SB}}(t; \lambda)$, respectively. Moreover, $\chi_{\text{SB}}(t)$, Eq. (3.2), is real, and so is the resultant $\tilde{\chi}_{\text{SB}}(i\varpi; \lambda)$, as highlighted in the last identity of Eq. (3.21). For its use in Eq. (3.20), the individual $\vartheta(\varpi)$ above is needed only for $\varpi \geq 0$. Mathematically, we would have

$$\vartheta(\varpi < 0) \equiv \vartheta(|\varpi|), \quad (3.23)$$

since the Matsubara poles in the upper/lower-half plane, $z = \pm i\varpi_n$, are symmetric.

Another remarkable property is the *equal area relation*:

$$\int_0^{\infty} d\omega \vartheta(\omega) = \int_0^{\infty} d\omega \varphi(\omega). \quad (3.24)$$

This arises from the formal consideration on the zero-temperature limit to Eq. (3.20), resulting in an integral, with the measure of $\varpi_{n+1}^{\pm} - \varpi_n^{\pm} = 2\pi/\beta$. Comparing the resultant $A_{\text{hyb}}^{\text{en}}$ with that of Eq. (3.5) or Eq. (3.16) leads to Eq. (3.24). Mathematically, one can view the above zero-temperature limit as a method of $\beta \rightarrow \infty$. It is concerned only with the β variable in the Fermi/Boson function $f_{\beta}^{\pm}(\omega)$. Remarkably, the equal-area relation (3.24) remains hold for general $\vartheta(\omega)$ and $\varphi(\omega)$, with temperature T dependence via parameters.

Note that in Eq. (3.20) the first term exists only for the bosonic case. It results from $1/(\beta\omega)$, the high-temperature term in the Bose function, evaluated by using^{11–13}

$$\tilde{\chi}_{\text{SB}}(0) = \tilde{\chi}_{\text{SB}}^{(r)}(0) = \frac{1}{\pi} \int_{-\infty}^{\infty} d\omega \frac{\tilde{\chi}_{\text{SB}}^{(i)}(\omega)}{\omega}. \quad (3.25)$$

The two identities arise from $\tilde{\chi}_{\text{SB}}^{(i)}(\omega = 0) = 0$ and the Kramers–Kronig relation, respectively.

It is worth re-emphasizing that Eq. (3.20) engages no contribution from the constant component of Bose/Fermi function. This is exact when the underlying spectral density $\varphi(\omega)$ is antisymmetric. While this requirement holds

naturally for the bosonic case, Eq. (3.6), the possibility of anti-symmetrization for the fermionic case has to be scrutinized and implemented, as Eqs. (3.11)–(3.17). Having the entanglement thermodynamic spectrum, $\vartheta(\varpi)$, been properly defined in Eqs. (3.21)–(3.23), the equal-area relation (3.24) does hold for both the bosonic and fermionic cases.

In Appendix, we present in detail the asymptotic analysis on the universal high-temperature thermodynamic behaviors. Again, Eq. (3.20) serves the convenient starting point for this analysis. We show the dramatic differences between the fermionic and bosonic hybridization scenarios, particularly in terms of the entropy changes.

IV. FERMIONIC ENTANGLEMENT THEORY WITH GAUSSIAN ENVIRONMENTS

A. Opening remarks

Consider hereafter the theoretical formulations with Gaussian bath environments. This is concerned with the standard coupling bath model, commonly used in open quantum systems. In this model, the bath h_{B} constitutes a collection of infinite noninteracting particles, either bosonic or fermionic, whereas the hybrid bath modes $\{\hat{F}_u\}$ are linear. The simplicity arises here due to the underlying Gaussian–Wick’s theorem.^{11–13} The influence of a Gaussian bath on an arbitrary system is completely dictated by the interacting spectral densities that are bare-bath subspace properties.

It is noticed that Gaussian environments go with the system–and–bath entanglement theory.³⁶ This theory relates the entangled response functions, such as $\chi_{\text{SB}}(t)$ of Eq. (3.1), to the local system properties, with any given bare-bath spectral densities. The corresponding relations for the entanglement free-energy spectral functions, $\varphi(\omega)$ and $\vartheta(\varpi)$ of Sec. III, will then be readily obtained. We defer the bosonic theory to Sec. V, where the existed nonentanglement $A_{\text{hyb}}^{\text{neb}}$, Eq. (2.8), will also be treated.

In this section, we present a comprehensive account on the system–bath entanglement theory with fermionic Gaussian coupling environments. The total composite Hamiltonian reads

$$H_{\text{T}} = H_{\text{S}} + h_{\text{B}} + \sum_u (\hat{a}_u^\dagger \hat{F}_u + \hat{F}_u^\dagger \hat{a}_u), \quad (4.1)$$

with

$$h_{\text{B}} = \sum_k \epsilon_k \hat{d}_k^\dagger \hat{d}_k \quad \text{and} \quad \hat{F}_u = \sum_k t_{uk}^* \hat{d}_k. \quad (4.2)$$

Here, \hat{d}_k^\dagger and \hat{a}_u^\dagger (\hat{d}_k and \hat{a}_u) are the creation (annihilation) operators for an electron in the specified bath state $|k\rangle$ of energy ϵ_k and system $|u\rangle$, respectively. The coupling parameter t_{uk} describes an electron transfer between $|u\rangle$ and $|k\rangle$ of a same spin. The local impurity system (H_{S}) is arbitrary, containing often open-shell elec-

trons with strong Coulomb interactions, under the influence of a fermionic coupling Gaussian environment.

As Sec. III B, we adopt the Green’s function convention for the fermionic theory. Note that in general

$$\begin{aligned} G_{AB}(t) &\equiv \langle \{\hat{A}(t), \hat{B}^\dagger(0)\} \rangle = G_{BA}^*(-t), \\ G_{AB}^*(t) &\equiv \langle \{\hat{A}^\dagger(t), \hat{B}(0)\} \rangle. \end{aligned} \quad (4.3)$$

Adopt also the convolution notation,

$$f_1(t) \otimes f_2(t) \equiv \int_0^t d\tau f_1(t - \tau) f_2(\tau). \quad (4.4)$$

Let $\tilde{f}(\omega)$ be the frequency resolution of $f(t)$, such as Eqs. (3.2) and (3.10),

$$\tilde{f}(\omega) \equiv \int_0^\infty dt e^{i\omega t} f(t). \quad (4.5)$$

We have $\tilde{f}(\omega) = \tilde{f}_1(\omega) \tilde{f}_2(\omega)$ if $f(t) = f_1(t) \otimes f_2(t)$.

Equation (4.2) constitutes a Gaussian environment, with the interacting bath spectral densities,

$$J_{uv}(\omega) = \pi \sum_k t_{uk}^* t_{vk} \delta(\omega - \epsilon_k). \quad (4.6)$$

Note that u and v appearing in pair carry a same spin, due to the aforementioned nature of transferring coupling parameter. From Eq. (4.2), we have

$$\hat{F}_u^{\text{B}}(t) \equiv e^{ih_{\text{B}}t} \hat{F}_{us} e^{-ih_{\text{B}}t} = \sum_k t_{uk}^* e^{-i\epsilon_k t} \hat{d}_k. \quad (4.7)$$

Together with $\{\hat{d}_k, \hat{d}_{k'}^\dagger\} = \delta_{kk'}$, we obtain

$$\langle \{\hat{F}_u^{\text{B}}(t), \hat{F}_v^\dagger\} \rangle = \sum_k t_{uk}^* t_{vk} e^{-i\epsilon_k t} = g_{uv}(t), \quad (4.8)$$

with $g_{uv}(t)$ being the interacting bath Green’s function that is formally defined as [cf. Eq. (4.3)]

$$g_{uv}(t) \equiv \langle \{\hat{F}_u^{\text{B}}(t), \hat{F}_v^{\text{B}\dagger}(0)\} \rangle_{\text{B}} = g_{vu}^*(-t). \quad (4.9)$$

One can then recast Eq. (4.6) as

$$J_{uv}(\omega) = \frac{1}{2} [\tilde{g}_{uv}(\omega) + \tilde{g}_{vu}^*(\omega)]. \quad (4.10)$$

Note that in Eq. (4.9), both $\hat{F}_u^{\text{B}}(t) \equiv e^{ih_{\text{B}}t} \hat{F}_{us} e^{-ih_{\text{B}}t}$ [Eq. (4.7)] and $\langle (\cdot) \rangle_{\text{B}} \equiv \text{tr}_{\text{B}}[(\cdot) e^{-\beta h_{\text{B}}}] / Z_0^{\text{B}}$, are defined in the bare-bath subspace, rather than the total composite space. In other words, $\hat{F}_u^{\text{B}}(t) \neq \hat{F}_u(t)$, except for $t = 0$, and $\langle (\cdot) \rangle_{\text{B}} \neq \langle (\cdot) \rangle$, unless it is a c-number in study.

B. System–bath entanglement theory

The system–bath entanglement theory is an input–output type of formalism. The inputs for the fermionic

theory below are $\mathbf{g}(t) \equiv \{g_{uv}(t)\}$, Eq. (4.9), and the local impurity Green's functions,

$$G_{uv}^{\text{SS}}(t) \equiv \langle \{\hat{a}_u(t), \hat{a}_v^\dagger(0)\} \rangle. \quad (4.11)$$

The outputs are the nonlocal Green's functions,

$$G_{uv}^{\text{BB}}(t) \equiv \langle \{\hat{F}_u(t), \hat{F}_v^\dagger(0)\} \rangle. \quad (4.12)$$

and

$$\begin{aligned} G_{uv}^{\text{SB}}(t) &\equiv \langle \{\hat{a}_u(t), \hat{F}_v^\dagger(0)\} \rangle, \\ G_{uv}^{\text{BS}}(t) &\equiv \langle \{\hat{F}_u(t), \hat{a}_v^\dagger(0)\} \rangle. \end{aligned} \quad (4.13)$$

Note that Eq. (3.8) can be recast in terms of these two quantities; see Eq. (4.26).

The theoretical development starts with the evaluation on $\hat{F}_u(t) \equiv e^{iH_{\text{T}}t} \hat{F}_u e^{-iH_{\text{T}}t}$, via the formal solution to

$$\dot{\hat{F}}_u = i[H_{\text{T}}, \hat{F}_u] = i[H_{\text{S}} + h_{\text{B}} + H_{\text{SB}}, \hat{F}_u]. \quad (4.14)$$

First of all, from Eqs. (4.1) and (4.2), we obtain

$$\dot{\hat{d}}_k = -i\epsilon_k \hat{d}_k - i \sum_v t_{vk} \hat{a}_v. \quad (4.15)$$

Its solution reads

$$\hat{d}_k(t) = e^{-i\epsilon_k t} \hat{d}_k(0) - i \int_0^t d\tau t_{vk} e^{-i\epsilon_k(t-\tau)} \hat{a}_v(\tau). \quad (4.16)$$

By applying it for \hat{F}_u in Eq. (4.2), followed by using Eqs. (4.7) and (4.8), we obtain [cf. Eq. (4.4)]

$$\hat{F}_u(t) = \hat{F}_u^{\text{B}}(t) - i \sum_v g_{uv}(t) \otimes \hat{a}_v(t). \quad (4.17)$$

It together with $\{\hat{F}_u^\dagger(t), \hat{a}_v^\dagger\} = 0$ via Eq. (4.7) result in

$$G_{uv}^{\text{BS}}(t) = -i \sum_{v'} g_{uv'}(t) \otimes G_{v'v}^{\text{SS}}(t). \quad (4.18)$$

The symmetry relation, Eq. (4.3), leads to further

$$G_{uv}^{\text{SB}}(t) = -i \sum_{v'} G_{uv'}^{\text{SS}}(t) \otimes g_{v'v}(t). \quad (4.19)$$

These identify the two output quantities of Eq. (4.13). Moreover, Eq. (4.17) together with Eq. (4.9) result in

$$G_{uv}^{\text{BB}}(t) = g_{uv}(t) - i \sum_{v'} g_{uv'}(t) \otimes G_{v'v}^{\text{SB}}(t). \quad (4.20)$$

Applying further Eq. (4.19) completes the output quantity in Eq. (4.12), with the input functions, Eqs. (4.9) and (4.11). In the matrix form, the above results are³⁶

$$\mathbf{G}^{\text{BB}}(t) = \mathbf{g}(t) - \mathbf{g}(t) \otimes \mathbf{G}^{\text{SS}}(t) \otimes \mathbf{g}(t), \quad (4.21)$$

and

$$\begin{aligned} \mathbf{G}^{\text{SB}}(t) &= -i \mathbf{G}^{\text{SS}}(t) \otimes \mathbf{g}(t), \\ \mathbf{G}^{\text{BS}}(t) &= -i \mathbf{g}(t) \otimes \mathbf{G}^{\text{SS}}(t). \end{aligned} \quad (4.22)$$

In terms of frequency resolutions, Eq. (4.5), they are

$$\tilde{\mathbf{G}}^{\text{BB}}(\omega) = \tilde{\mathbf{g}}(\omega) - \tilde{\mathbf{g}}(\omega) \tilde{\mathbf{G}}^{\text{SS}}(\omega) \tilde{\mathbf{g}}(\omega). \quad (4.23)$$

and

$$\begin{aligned} \tilde{\mathbf{G}}^{\text{SB}}(\omega) &= -i \tilde{\mathbf{G}}^{\text{SS}}(\omega) \tilde{\mathbf{g}}(\omega), \\ \tilde{\mathbf{G}}^{\text{BS}}(\omega) &= -i \tilde{\mathbf{g}}(\omega) \tilde{\mathbf{G}}^{\text{SS}}(\omega). \end{aligned} \quad (4.24)$$

These two matrixes are of equal trace, with

$$\text{tr} \tilde{\mathbf{G}}^{\text{SB}}(\omega) = \text{tr} \tilde{\mathbf{G}}^{\text{BS}}(\omega) = -i \text{tr} [\tilde{\mathbf{g}}(\omega) \tilde{\mathbf{G}}^{\text{SS}}(\omega)]. \quad (4.25)$$

C. Thermodynamic spectral functions with fermionic Gaussian environments

It is noticed that, by using Eq. (4.13), we can recast Eq. (3.8) as $G_{\text{SB}}(t) = \text{tr} \mathbf{G}^{\text{SB}}(t) + \text{tr} \mathbf{G}^{\text{BS}}(t)$. Together with Eq. (4.25), we obtain

$$\tilde{G}_{\text{SB}}(\omega) = -2i \text{tr} [\tilde{\mathbf{g}}(\omega) \tilde{\mathbf{G}}^{\text{SS}}(\omega)]. \quad (4.26)$$

This is the basis for revisiting various entanglement thermodynamic spectral functions, defined in Sec. III, with the fermionic Gaussian environments.

Let us start with the form of $\tilde{G}_{\text{SB}}(\omega; \lambda)$ via Eq. (4.26). As inferred from Eq. (4.9), $\tilde{\mathbf{g}}(\omega; \lambda) = \lambda^2 \tilde{\mathbf{g}}(\omega)$. Therefore,

$$\tilde{G}_{\text{SB}}(\omega; \lambda) = -2i \lambda^2 \text{tr} [\tilde{\mathbf{g}}(\omega) \tilde{\mathbf{G}}^{\text{SS}}(\omega; \lambda)]. \quad (4.27)$$

The free-energy spectral functions, Eqs. (3.17) and (3.22), are then ($\varpi \geq 0$)

$$\varphi(\omega) = -\frac{1}{2} \text{Im} \int_0^1 d\lambda^2 [X(\omega; \lambda) - X(-\omega; \lambda)], \quad (4.28)$$

$$\vartheta(\varpi) = -\text{Re} \int_0^1 d\lambda^2 \text{tr} [\tilde{\mathbf{g}}(i\varpi) \tilde{\mathbf{G}}^{\text{SS}}(i\varpi; \lambda)], \quad (4.29)$$

where

$$X(\omega; \lambda) \equiv \text{tr} [\tilde{\mathbf{g}}(\omega) \tilde{\mathbf{G}}^{\text{SS}}(\omega; \lambda)]. \quad (4.30)$$

Note that $\tilde{\mathbf{G}}^{\text{SS}}(\omega; \lambda)$ is an even function of λ .

Let us repeat the two equivalent free-energy expressions, Eq. (3.16) and Eq. (3.20) for the fermionic case, as follows.

$$A_{\text{hyb}}(T) = -\frac{1}{\pi} \int_{-\infty}^{\infty} d\omega \frac{\varphi(\omega)}{1 + e^{\beta\omega}} = \frac{2}{\beta} \sum_{n=1}^{\infty} \vartheta(\varpi_n), \quad (4.31)$$

with $\{\varpi_n = (2n-1)\pi/\beta\}$, the fermionic Matsubara frequencies. Note that in the fermionic hybridization scenario, $A_{\text{hyb}}(T) = A_{\text{hyb}}^{\text{en}}(T)$ [cf. Eq. (2.12)]. Moreover, the spectral density $\varphi(\omega)$ and the corresponding spectrum $\vartheta(\omega)$ are of equal area [Eq. (3.24)] within $\omega \in [0, \infty)$.

Remarkably, the above formalism implies the thermodynamics of quantum impurity systems be measurable. First of all, it is exact with the Gaussian environment

ansatz that is well satisfied in the thermodynamic limit. For quantum impurity systems, such as quantum dots, one could continuously adjust λ the system–bath coupling strength.^{55–60} One can also measure the impurity spectral densities,^{61,62} resulting in the local Green’s function, $\tilde{\mathbf{G}}^{\text{ss}}(\omega; \lambda)$. Another ingredient $\tilde{\mathbf{g}}(\omega)$ in Eq. (4.27) is dictated by the bare–bath hybridization, $\{J_{uv}(\omega)\}$ of Eq. (4.10), that could be determined with various accurate methods. The above formalism would imply that the thermodynamics of fermionic quantum impurity systems be measurable in experiments.

V. BOSONIC ENTANGLEMENT THEORY WITH GAUSSIAN ENVIRONMENTS

A. Nonentanglement contribution

It is worth reminding that in the bosonic case, the nonentanglement component, $A_{\text{hyb}}^{\text{nen}} \equiv A_{\text{hyb}} - A_{\text{hyb}}^{\text{en}}$, Eq. (2.8), is nonzero in general, except for noninteracting systems (cf. Sec. VI A). The bosonic theory presented below, in parallel to Sec. IV, will naturally treat not only the entanglement component,³⁶ but also the nonentanglement part. This is concerned with relating the mean values of hybrid bath operators, $\{\langle \hat{F}_u \rangle\}$, to those local system dissipative modes, $\{\langle \hat{Q}_u \rangle\}$; see Eq. (5.6).

Let us start with the bosonic counterpart to Eq. (4.8),

$$i[\hat{F}_u^{\text{B}}(t), \hat{F}_v(0)] = i[\hat{F}_u^{\text{B}}(t), \hat{F}_v^{\text{B}}(0)] \equiv \phi_{uv}(t). \quad (5.1)$$

This commutator itself is a c-number and equals to the bare–bath response function [cf. Eq. (4.9)],

$$\phi_{uv}(t) = i\langle [\hat{F}_u^{\text{B}}(t), \hat{F}_v^{\text{B}}(0)] \rangle_{\text{B}}. \quad (5.2)$$

As any response function between two Hermitian operators, $\phi_{uv}(t)$ is real, satisfying $\phi_{vu}(-t) = -\phi_{uv}(t)$. The bare–bath spectral density is given by [cf. Eq. (4.10)]

$$J_{uv}(\omega) = \frac{1}{2}[\tilde{\phi}_{uv}(\omega) - \tilde{\phi}_{vu}(-\omega)]. \quad (5.3)$$

Denote for the use soon below

$$\eta_{uv} \equiv \int_0^\infty dt \phi_{uv}(t) = \tilde{\phi}_{uv}(\omega = 0). \quad (5.4)$$

The bosonic counterpart to Eq. (4.17) reads

$$\hat{F}_u(t) = \hat{F}_u^{\text{B}}(t) - \sum_v \phi_{uv}(t) \otimes \hat{Q}_v(t). \quad (5.5)$$

This immediately results in

$$\langle \hat{F}_u \rangle = - \sum_v \eta_{uv} \langle \hat{Q}_v \rangle. \quad (5.6)$$

We can also obtain this interesting result via the DEOM theory that is exact with Gaussian environments.^{30,31} The nonentanglement term in Eq. (2.7) becomes

$$\langle H_{\text{SB}} \rangle^{\text{nen}} = \sum_u \langle \hat{Q}_u \rangle \langle \hat{F}_u \rangle = - \sum_{uv} \eta_{uv} \langle \hat{Q}_u \rangle \langle \hat{Q}_v \rangle. \quad (5.7)$$

Note also that $\tilde{\phi}_{uv}(\omega; \lambda) = \lambda^2 \tilde{\phi}_{uv}(\omega)$. Consequently, Eq. (5.7) leads to the nonentanglement free–energy contribution, Eq. (2.8), the final expression of

$$A_{\text{hyb}}^{\text{nen}}(T) = -\frac{1}{2} \sum_{uv} \eta_{uv} \int_0^1 d\lambda^2 \langle \hat{Q}_u \rangle_\lambda \langle \hat{Q}_v \rangle_\lambda. \quad (5.8)$$

The individual $\langle \hat{Q}_u \rangle_\lambda$ is an even function of λ .

B. Entanglement contribution

As specified earlier, the entanglement thermodynamics can be described in terms of thermodynamic spectral functions, $\varphi(\omega)$ [Eq. (3.6)] and $\vartheta(\varpi)$ [Eq. (3.21)]. This description is rooted at the system–and–bath symmetrized response function, $\chi_{\text{SB}}(t)$ of Eq. (3.1). The inputs for its evaluation via the entanglement theory are the bare–bath $\phi(t) \equiv \{\phi_{uv}(t)\}$ and the local–system response functions [cf. Eq. (4.11)],

$$\chi_{uv}^{\text{SS}}(t) \equiv i\langle [\hat{Q}_u(t), \hat{Q}_v(0)] \rangle. \quad (5.9)$$

The outputs, especially those relevant to entanglement thermodynamics, are the following two nonlocal response functions [cf. Eq. (4.13)],

$$\begin{aligned} \chi_{uv}^{\text{SB}}(t) &\equiv i\langle [\hat{Q}_u(t), \hat{F}_v(0)] \rangle, \\ \chi_{uv}^{\text{BS}}(t) &\equiv i\langle [\hat{F}_u(t), \hat{Q}_v(0)] \rangle. \end{aligned} \quad (5.10)$$

The bosonic system–bath entanglement theorem reads³⁶

$$\begin{aligned} \tilde{\chi}^{\text{SB}}(\omega) &= -\tilde{\chi}^{\text{SS}}(\omega) \tilde{\phi}(\omega), \\ \tilde{\chi}^{\text{BS}}(\omega) &= -\tilde{\phi}(\omega) \tilde{\chi}^{\text{SS}}(\omega). \end{aligned} \quad (5.11)$$

These two matrixes are of equal trace, with

$$\text{tr} \tilde{\chi}^{\text{SB}}(\omega) = \text{tr} \tilde{\chi}^{\text{BS}}(\omega) = -\text{tr}[\tilde{\phi}(\omega) \tilde{\chi}^{\text{SS}}(\omega)]. \quad (5.12)$$

Apparently, Eqs. (5.11) and (5.12) are the bosonic counterparts to Eqs. (4.24) and (4.25), respectively.

Moreover, by using Eq. (5.10), we can recast Eq. (3.1) as $\chi_{\text{SB}}(t) = \frac{1}{2}[\text{tr} \tilde{\chi}^{\text{SB}}(\omega) + \text{tr} \tilde{\chi}^{\text{BS}}(\omega)]$, resulting in

$$\chi_{\text{SB}}(t) = -\text{tr}[\tilde{\phi}(\omega) \tilde{\chi}^{\text{SS}}(\omega)]. \quad (5.13)$$

We obtain [cf. Eq. (4.27)]

$$\tilde{\chi}_{\text{SB}}(\omega; \lambda) = -\lambda^2 \text{tr}[\tilde{\phi}(\omega) \tilde{\chi}^{\text{SS}}(\omega; \lambda)]. \quad (5.14)$$

The resultant Eqs. (3.6) and (3.21) read ($\varpi \geq 0$)

$$\varphi(\omega) = \frac{1}{2} \text{Im} \int_0^1 d\lambda^2 \text{tr}[\tilde{\phi}(\omega) \tilde{\chi}^{\text{SS}}(\omega; \lambda)], \quad (5.15)$$

$$\vartheta(\varpi) = \frac{1}{2} \int_0^1 d\lambda^2 \text{tr}[\tilde{\phi}(i\varpi) \tilde{\chi}^{\text{SS}}(i\varpi; \lambda)]. \quad (5.16)$$

Let us repeat Eqs. (3.5) and (3.20) for the bosonic case below:

$$\begin{aligned} A_{\text{hyb}}^{\text{en}}(T) &= -\frac{1}{\pi} \int_{-\infty}^{\infty} d\omega \frac{\varphi(\omega)}{1 - e^{-\beta\omega}} \\ &= -\frac{1}{\beta} \vartheta(0) - \frac{2}{\beta} \sum_{n=1}^{\infty} \vartheta(\varpi_n), \end{aligned} \quad (5.17)$$

with $\{\varpi_n = 2n\pi/\beta\}$ being the bosonic Matsubara frequencies. See also Eq. (3.24) for the equal area of $\varphi(\omega)$ and $\vartheta(\omega)$, within $\omega \in [0, \infty)$.

Combining Eq. (5.8), we obtain the hybridizing free-energy, $A_{\text{hyb}}(T) = A_{\text{hyb}}^{\text{en}}(T) + A_{\text{hyb}}^{\text{en}}(T)$, in terms of the local properties, $\langle \hat{Q}_u \rangle_\lambda$ and $\tilde{\chi}_{uv}^{\text{ss}}(\omega; \lambda)$, and the bare-bath $\tilde{\phi}_{uv}(\omega)$ or $J_{uv}(\omega)$ of Eq. (5.3). The above formalism would imply that the thermodynamics of bosonic quantum impurity systems be also experimentally measurable. Again, the key issues would be the tunability with respect to the system-bath coupling strength.^{55–60}

VI. ANALYTICAL RESULTS VERSUS GENERAL REMARKS

In this section, we present the concrete illustrations with noninteracting systems. However, we will also deduce some nontrivial insides for thermodynamics of arbitrary fermionic systems. There are a number of striking different features from their bosonic counterparts. We thoroughly address those puzzles in study with the underlying physical principles.

A. Brownian oscillator systems

The simplest noninteracting bosonic scenario is the one-dimensional Brownian oscillator (BO) system. This is concerned with a local harmonic oscillator of frequency ω_s and (dimensionless) coordinate \hat{q}_s , embedded in a Gaussian environment. The system-bath coupling is described with $H_{\text{SB}} = \hat{q}_s \hat{F}$; i.e., $\hat{Q}_s = \hat{q}_s$ here. For the BO complex, $\langle \hat{q}_s \rangle = 0$; thus the nonentanglement $A_{\text{hyb}}^{\text{en}} = 0$ via Eq. (5.8).

The BO system is analytically solvable. The resultant local-system susceptibility function reads^{11–13}

$$\tilde{\chi}_{\text{ss}}(\omega) = \frac{\omega_s}{\omega_s^2 - \omega^2 - \omega_s \tilde{\phi}(\omega)}, \quad (6.1)$$

with $\tilde{\phi}(\omega)$ being the frequency resolution on the interacting bath response function, $\phi(t)$ of Eq. (5.2). Note that

$$\tilde{\chi}_{\text{SB}}(\omega) = -\tilde{\phi}(\omega) \tilde{\chi}_{\text{ss}}(\omega). \quad (6.2)$$

Moreover,

$$\tilde{\chi}_{\text{SB}}(\omega; \lambda) = -\frac{\lambda^2 \omega_s \tilde{\phi}(\omega)}{\omega_s^2 - \omega^2 - \lambda^2 \omega_s \tilde{\phi}(\omega)}. \quad (6.3)$$

The resultant Eqs. (5.15) and (5.16), respectively, are given by ($\varpi \geq 0$)

$$\varphi(\omega) = \frac{1}{2} \text{Im} \{ \ln [1 + \phi(\omega) \tilde{\chi}_{\text{ss}}(\omega)] \}, \quad (6.4)$$

$$\vartheta(\varpi) = \frac{1}{2} \ln |1 + \phi(i\varpi) \tilde{\chi}_{\text{ss}}(i\varpi)|. \quad (6.5)$$

Interestingly, the free-energy spectral density, $\varphi(\omega)$, is just the half-phase of $1 + \phi(i\varpi) \tilde{\chi}_{\text{ss}}(i\varpi) = 1 - \tilde{\chi}_{\text{SB}}(\omega)$, whereas the Laplacian spectrum, $\vartheta(\varpi)$, is the half-exponent of $|1 - \tilde{\chi}_{\text{SB}}(i\varpi)|$. It is worth noting that the above characteristics are limited to noninteracting systems. Equation (6.5) reads explicitly

$$\vartheta(\varpi \geq 0) = \frac{1}{2} \ln \left| \frac{\omega_s^2 + \varpi^2}{\omega_s^2 + \varpi^2 - \omega_s \tilde{\phi}(i\varpi)} \right|. \quad (6.6)$$

This is a continuous and even function; cf. Eq. (3.23).

On the other hand, $\varphi(\omega)$ of Eq. (6.4), which is an odd function [$\varphi(-\omega) = -\varphi(\omega)$], is related to the aforementioned phase property, with the discontinuity (for $\omega > 0$):

$$\varphi(\omega \neq \omega_s) = \frac{1}{2} \arg \left[\frac{\omega_s^2 - \omega^2}{\omega_s^2 - \omega^2 - \omega_s \tilde{\phi}(\omega)} \right], \quad (6.7a)$$

$$\varphi(\omega = \omega_s - 0^+) = -\frac{1}{2} \arg[\tilde{\phi}(\omega_s)] + \frac{\pi}{2}, \quad (6.7b)$$

$$\varphi(\omega = \omega_s + 0^+) = -\frac{1}{2} \arg[\tilde{\phi}(\omega_s)]. \quad (6.7c)$$

The discontinuity occurs at the BO frequency, $\omega = \omega_s$. This is a feature of noninteracting systems. The observed $\pi/2$ jump in $\varphi(\omega)$, at $\omega = \omega_s \pm 0^+$, arises from the π -shift in the phase of $[1 + \tilde{\phi}(\omega) \tilde{\chi}_{\text{ss}}(\omega)]$, as implied in Eq. (6.4).

B. Fermionic Brownian oscillator

The simplest noninteracting fermionic case is concerned with a spinless-dot electronic system, $\hat{H}_s = \epsilon_s \hat{a}^\dagger \hat{a}$, with a transfer coupling, $H_{\text{SB}} = \hat{a}^\dagger \hat{F} + \hat{F}^\dagger \hat{a}$, to a noninteracting electron reservoir environment. Evaluate the Heisenberg equation of motion for the system, resulting in $\dot{\hat{a}}(t) = -i\epsilon_s \hat{a}(t) - i\hat{F}(t)$. By using Eq. (4.17), we obtain $\hat{a}(t) = -i\epsilon_s \hat{a}(t) - g(t) \otimes \hat{a}(t) - i\hat{F}^{\text{B}}(t)$, and further $\dot{G}_{\text{ss}}(t) = -i\epsilon_s G_{\text{ss}}(t) - g(t) \otimes G_{\text{ss}}(t)$. Note that the initial value of $G_{\text{ss}}(t) = 1$. We obtain the well-known result of

$$\tilde{G}_{\text{ss}}(\omega) = \frac{i}{\omega - \epsilon_s + i\tilde{g}(\omega)}. \quad (6.8)$$

Note that [cf. Eq. (4.26)]

$$\tilde{G}_{\text{SB}}(\omega) = -2i\tilde{g}(\omega) \tilde{G}_{\text{ss}}(\omega). \quad (6.9)$$

The λ -augmented correspondence is then [cf. Eq. (6.3)]

$$\tilde{G}_{\text{SB}}(\omega; \lambda) = \frac{2\lambda^2 \tilde{g}(\omega)}{\omega - \epsilon_s + i\lambda^2 \tilde{g}(\omega)}. \quad (6.10)$$

Perform the thermodynamic integration and obtain Eqs. (3.17) and (3.22) the expressions ($\varpi \geq 0$),

$$\varphi(\omega) = \frac{1}{2} \text{Im} \left\{ \ln \left[\frac{1 - \tilde{g}(\omega) \tilde{G}_{\text{SS}}(\omega)}{1 - \tilde{g}(-\omega) \tilde{G}_{\text{SS}}(-\omega)} \right] \right\}, \quad (6.11)$$

$$\vartheta(\varpi) = \ln |1 - \tilde{g}(i\varpi) \tilde{G}_{\text{SS}}(i\varpi)|. \quad (6.12)$$

The last expression reads explicitly

$$\vartheta(\varpi \geq 0) = \ln \left| \frac{i\varpi - \epsilon_{\text{S}}}{i\varpi - \epsilon_{\text{S}} + i\tilde{g}(i\varpi)} \right|. \quad (6.13)$$

This is a continuous and even function.

In contrast, the phase, $\varphi(\omega)$ of Eq. (6.11), is an odd function and discontinued at $\omega = \pm\omega_{\text{S}}$, with $\omega_{\text{S}} \equiv |\epsilon_{\text{S}}|$ and the following explicit form (for $\omega \geq 0$):

$$\varphi(\omega \neq \omega_{\text{S}}) = \frac{1}{2} \arg \left[\frac{1 - \tilde{g}(\omega) \tilde{G}_{\text{SS}}(\omega)}{1 - \tilde{g}(-\omega) \tilde{G}_{\text{SS}}(-\omega)} \right], \quad (6.14a)$$

$$\varphi(\omega = \omega_{\text{S}} - 0^+) = \frac{1}{2} \arg \left[\frac{i\tilde{g}(-\omega_{\text{S}})}{2\omega_{\text{S}} + i\tilde{g}(\omega_{\text{S}})} \right], \quad (6.14b)$$

$$\varphi(\omega = \omega_{\text{S}} + 0^+) = \frac{1}{2} \arg \left[\frac{i\tilde{g}(-\omega_{\text{S}})}{2\omega_{\text{S}} + i\tilde{g}(\omega_{\text{S}})} \right] - \frac{\pi}{2}. \quad (6.14c)$$

Note that $\omega_{\text{S}} \equiv |\epsilon_{\text{S}}|$. Moreover, $\varphi(-\omega) = -\varphi(\omega)$, the anti-symmetrization as implied in Eq. (3.17), whereas Eq. (6.14) describes only $\varphi(\omega > 0)$. The discontinuity occurs at $\omega_{\text{S}} \pm 0^+$, at which $\varphi(\omega)$ is subject to a $\pi/2$ -phase jump.

C. Numerical demonstrations and discussions

For their dictating the thermodynamic spectral functions, we would also like to show the response/Green's functions. The bosonic case involves $\tilde{\chi}_{\text{SS}}(\omega)$ and $\tilde{\chi}_{\text{SB}}(\omega)$, whereas the fermionic case goes by $\tilde{X}_{\text{SS}}(\omega)$ and $\tilde{X}_{\text{SB}}(\omega)$. On the other hand, while $\chi_{\text{SS}}(t)$ and $\chi_{\text{SB}}(t)$ are real, $G_{\text{SS}}(\omega)$ and $G_{\text{SB}}(\omega)$ are complex. For the purpose of one-to-one comparison, we set

$$X_{\text{SS}}(t) = \frac{i}{2} [G_{\text{SS}}(t) - G_{\text{SS}}(-t)] = -\text{Im}G_{\text{SS}}(t). \quad (6.15)$$

$$X_{\text{SB}}(t) = \frac{i}{2} [G_{\text{SB}}(t) - G_{\text{SB}}(-t)] = -\text{Im}G_{\text{SB}}(t). \quad (6.16)$$

Consequently, the real parts of $\tilde{\chi}_{\text{SS}}(\omega)$, $\tilde{\chi}_{\text{SB}}(\omega)$, $\tilde{X}_{\text{SS}}(\omega)$ and $\tilde{X}_{\text{SB}}(\omega)$ are odd functions, whereas their imaginary parts are even ones. In fact, $\tilde{X}_{\text{SB}}^{(i)}(\omega) = \mathcal{J}_{\text{SB}}^{\text{odd}}(\omega)$ of Eq. (3.14) or the antisymmetrized $\text{Im}X(\omega; \lambda = 1)$ of Eq. (4.30). Note also that the spectral functions, $\varphi(\omega)$ and $\vartheta(\omega = \varpi)$, are odd and even functions, respectively.

Presented in Fig. 1 and Fig. 2 are the calculated results on the bosonic and fermionic cases, respectively. Those even functions are in red and the odd ones are in black. Adopt for the demonstrations a Drude bath model,

$$\tilde{\phi}(\omega) = \frac{i\eta\gamma}{\omega + i\gamma} = \tilde{g}(\omega), \quad (6.17)$$

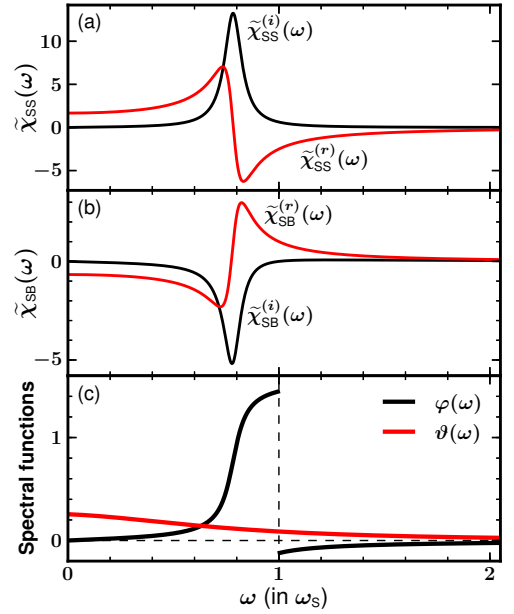


FIG. 1: Results on a bosonic BO with a Drude environment. (a) Local system $\tilde{\chi}_{\text{SS}}(\omega)$ [Eq. (6.1)], in unit of ω_{S}^{-1} , with the BO system frequency ω_{S} ; (b) Nonlocal $\tilde{\chi}_{\text{SB}}(\omega)$ [Eq. (6.2)]; (c) Spectral functions, $\varphi(\omega)$ [black; Eq. (6.7)] and $\vartheta(\varpi = \omega)$ [red; Eq. (6.5)]. See text for the environment parameters.

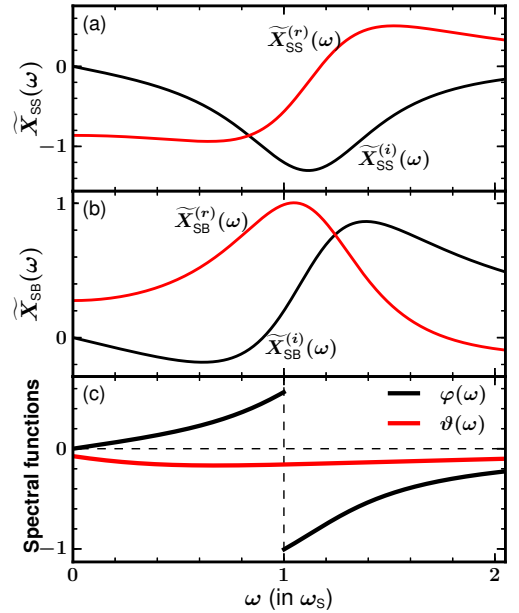


FIG. 2: The fermionic counterparts to those in Fig. 1. (a) The resultant local $\tilde{X}_{\text{SS}}(\omega)$ [cf. Eq. (6.15)], in unit of ω_{S}^{-1} . The system energy is negative, located at $\epsilon_{\text{S}} = -\omega_{\text{S}}$; (b) Nonlocal $\tilde{X}_{\text{SB}}(\omega)$ [cf. Eq. (6.16)]; (c) Spectral functions, $\vartheta(\omega)$ [black; Eq. (6.13)] and $\varphi(\varpi = \omega)$ [red; Eq. (6.14)].

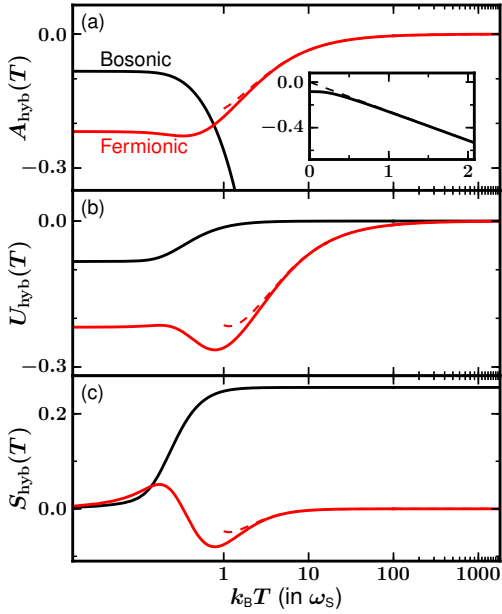


FIG. 3: Thermodynamic properties: (a) Hybridization free-energy $A_{\text{hyb}}(T)$, in unit of ω_s ; (b) Internal energy $U_{\text{hyb}}(T)$, in unit of ω_s ; (c) Entropy $S_{\text{hyb}}(T)$, in unit of k_B , for the bosonic (black) and fermionic (red) BO systems of Fig. 1 and Fig. 2, respectively.

with $\eta = 0.4\omega_s$ and $\gamma = 4\omega_s$, for both the bosonic and fermionic BO systems. The bosonic BO is of the frequency ω_s . The fermionic BO is of the local on-site energy, $\epsilon_s = -\omega_s$, below the Fermi energy of electronic bath reservoir.

Reported in Fig. 3 are the hybridization (a) free-energy $A_{\text{hyb}}(T)$, (b) internal energy $U_{\text{hyb}}(T)$, and (c) entropy $S_{\text{hyb}}(T)$, for both the bosonic (black) and fermionic (red) noninteracting systems. The inset in Fig. 3(a) depicts the linear-plot on bosonic $A_{\text{hyb}}(T)$. Included is also its high-temperature asymptotics, $-k_B T \vartheta(0)$ (dot); see Eq. (5.17) or Eq. (6.18a). The observed $A_{\text{hyb}}(T) < 0$ indicates the isotherm processes are spontaneous, in both the bosonic and fermionic cases.

We have numerically confirmed the identities in individual Eq. (4.31) and Eq. (5.17), for both the bosonic and fermionic cases, and also the equal-area relation (3.24). The negative amplitude of the area amounts to the value of $A_{\text{hyb}}(T = 0)$. The resultant $S_{\text{hyb}}(T = 0) = 0$ would also be general, for its agreeing with the Third Law.

Interestingly, the BO systems, bosonic versus fermionic, show remarkably distinct behaviors in their thermodynamic functions, especially the hybridization entropy, $S_{\text{hyb}}(T)$. These will be elaborated together with their high-temperature thermodynamic characteristics, as follows.

The bosonic BO hybridization is both energetically and entropically favored, with $U_{\text{hyb}}(T) < 0$ and $S_{\text{hyb}}(T) > 0$, at all temperatures. Moreover, in the high-temperature

regime, we have [cf. Eq. (A.1)]

$$\lim_{T \rightarrow \infty} \frac{A_{\text{hyb}}(T)}{k_B T} = -\vartheta(0), \quad (6.18a)$$

$$S_{\text{hyb}}(T \rightarrow \infty) = k_B \vartheta(0), \quad (6.18b)$$

$$U_{\text{hyb}}(T \rightarrow \infty) = 0. \quad (6.18c)$$

This is an ideal hybridization scenario. In other words, in the high-temperature limit, the bosonic BO mixtures are ideal solutions in the elementary physical chemistry. The observed $U_{\text{hyb}}(T) < U_{\text{hyb}}(T \rightarrow \infty)$ reflects the quantum effect. It seems as if Eq. (6.18) were specialized for noninteracting bosonic complexes, where $A_{\text{hyb}}^{\text{en}} = A_{\text{hyb}}$ and $\partial\vartheta/\partial T = 0$. However, we would argue, to the end of this section, that Eq. (6.18) be universal for arbitrary bosonic systems in the limit of $T \rightarrow \infty$.

It is worth noting that, for the bosonic noninteracting case, $A_{\text{hyb}}(T)$, $U_{\text{hyb}}(T)$ and $S_{\text{hyb}}(T)$ are all monotonic functions. None of them shows the turnover behavior. This would not be true for anharmonic systems, such as the spin-boson complex, with these three thermodynamic functions being evaluated via a numerically accurate method.⁵⁴

Turn to the fermionic case, the red-curves in Fig. 3. First of all, we have Eq. (A.2) for the fermionic case in general. That is [cf. Eq. (6.18)]

$$A_{\text{hyb}}(\infty) = S_{\text{hyb}}(\infty) = U_{\text{hyb}}(\infty) = 0. \quad (6.19)$$

These are universal fermionic relations in the limit of $T \rightarrow \infty$. We will discuss the physical picture to the end of this section, together with that of the bosonic Eq. (6.18).

Note that for noninteracting systems, the thermodynamic spectrum is temperature-independent. That is $\partial\vartheta(\varpi)/\partial\beta = 0$. The resultant Eq. (A.18), together with Eq. (A.5), read

$$A_{\text{hyb}}(T) \approx \frac{\kappa_a}{\xi_a} \varpi_a \vartheta(\varpi_a), \quad (6.20a)$$

$$U_{\text{hyb}}(T) \approx -\frac{\kappa_a}{\xi_a} \varpi_a^2 \vartheta'(\varpi_a), \quad (6.20b)$$

$$S_{\text{hyb}}(T) \approx -\frac{\kappa_a}{\xi_a T} [\varpi_a \vartheta(\varpi_a) + \varpi_a^2 \vartheta'(\varpi_a)]. \quad (6.20c)$$

Here $\kappa_a = 3$, $\xi_a = \sqrt{12}$ and $\varpi_a = \xi_a/\beta$ [Eq. (A.19)], arising from the simplest Padé the [0/1]-approximant of Fermi function.⁶³⁻⁶⁵ Note that $\vartheta'(\varpi) \equiv d\vartheta(\varpi)/d\varpi$. Included in Fig. 3 are also the high-temperature approximants, Eq. (6.20), with the red-curves for $k_B T/\omega_s > 1$. The accuracy is up to at least the order of $\mathcal{O}[(\beta\omega_s)^3]$, as inferred from Eq. (A.17). Note that the local system energy is $\epsilon_s = -\omega_s$, below the Fermi energy of bath environment. However, we can analytically prove that the sign of ϵ_s does not affect $\vartheta(\varpi)$ in the present study.

Strikingly, none of the fermionic $A_{\text{hyb}}(T)$, $U_{\text{hyb}}(T)$ and $S_{\text{hyb}}(T)$ is monotonic. In particular, the fermionic $S_{\text{hyb}}(T)$ shows a double-turnover characteristics. The first one occurs in the entropically favored region, with the maximum $S_{\text{hyb}}^{\text{max}}(T) > 0$. As temperature increases,

$S_{\text{hyb}}(T)$ drops, getting into the entropically unfavored region, where the second turnover occurs, with the minimum $S_{\text{hyb}}^{\text{min}}(T) < 0$. Afterward, it increases toward $S_{\text{hyb}}(T \rightarrow \infty) \rightarrow 0$. It is noticed that the bosonic $A_{\text{hyb}}(T)$, $U_{\text{hyb}}(T)$ and $S_{\text{hyb}}(T)$ consist only of turns, occurring right in the temperature region where seen the fermionic counterparts turnovers. Therefore, we could attribute the observed turnovers to the interplay between system energy, thermal bath fluctuations and the Pauli exclusion principle.

To close this section, we would like to address the physical picture behind the bosonic Eq. (6.18) and fermionic Eq. (6.19). Both comprise the universal relations in the limit of $T \rightarrow \infty$. In particular, the observed $U_{\text{hyb}}(T \rightarrow \infty) = 0$ in both bosonic and fermionic cases agree perfectly with the classical energy equipartition theorem. The total number of degree of freedom is invariant upon hybridization. This observation explains also the fermionic $S_{\text{hyb}}(T \rightarrow \infty) = 0$. The *fermionic entropy equipartition theorem* is the maximum qubit entropy of $k_B \ln 2$ for each fermion. This together with the aforementioned energy equipartition theorem result in further the fermionic $A_{\text{hyb}}(T \rightarrow \infty) = 0$. Interestingly, the fermionic entropy equipartition theorem gives also rise to the observed fermionic $S_{\text{hyb}}(T) < 0$ in the high-temperature regime, as it increases toward $S_{\text{hyb}}(T \rightarrow \infty) = 0$. In this regime, the Pauli exclusion results in a lyophobic complex, with $U_{\text{hyb}}(T) < 0$ and $S_{\text{hyb}}(T) < 0$, prior to the equipartition theorem takes the place.

VII. CONCLUDING REMARKS

In summary, we have presented a comprehensive theory of thermodynamics in the quantum regime. Both the bosonic and fermionic hybridization scenarios are considered. We identify thermodynamic spectral functions, together with the underlying relations (Sec. III and Appendix). By exploiting the system-bath entanglement theory, we further relate the thermodynamic spectral functions to experimental measurable quantities (Sec. IV and Sec. V).

It is noticed that there are two types of thermodynamic spectral functions: The free-energy spectral density, $\varphi(\omega)$ [Eq. (3.6) or Eq. (3.17)], and the thermodynamic spectrum, $\vartheta(\varpi)$ [Eq. (3.21) or Eq. (3.22)]. The former is defined in the Fourier frequency domain with odd parity. The latter is in the Laplacian frequency domain with even parity. Each of them completely characterizes the entanglement thermodynamics properties. Nevertheless, we would suggest the thermodynamic spectrum formalism be the choice of convenience.

We further show some remarkably different thermodynamic characteristics between the bosonic and fermionic noninteracting systems. These provide the solid references for the future studies on strongly correlated impurity complexes, by using the general theories developed in

this work. It is worth reemphasizing the fact that both the bosonic Eq. (6.18) and the fermionic Eq. (6.19) are universal in the high-temperature limit. We attribute these limiting results to the equipartition theorem, as stipulated to the end of Sec. VI.

It is noticed that the current state-of-the-art devices available for quantum simulation include quantum dots, cold atoms/trapped ions, superconducting circuits, etc.⁵⁵⁻⁶⁰ The established technologies on manipulating such as the coupling conjunctions could be exploited for the required thermodynamic λ -integral here. Therefore, the theoretical findings of this work would constitute a crucial component for thermodynamics in the quantum regime being measurable in experiments.

Acknowledgments

The support from the Ministry of Science and Technology (Nos. 2016YFA0400900, 2016YFA0200600 and 2017YFA0204904) the Natural Science Foundation of China (Nos. 21633006, 21703225 and 21973086) is gratefully acknowledged.

Appendix: High-temperature regime: Bosonic versus fermionic scenarios

This appendix presents the high-temperature characteristics of entanglement thermodynamic functions. We will see there are dramatic differences between the bosonic and fermionic hybridization cases. Note that $A_{\text{hyb}}^{\text{en}}(T) = U_{\text{hyb}}^{\text{en}}(T) - TS_{\text{hyb}}^{\text{en}}(T)$. The hybridization entropy is $S_{\text{hyb}}^{\text{en}}(T) = -\partial A_{\text{hyb}}^{\text{en}}(T)/\partial T$.

Consider the bosonic case, $A_{\text{hyb}}^{\text{en}}(T)$ of Eq. (3.20). The first term there, $-k_B T \vartheta(0)$, dominates the high-temperature properties. We obtain

$$A_{\text{hyb}}^{\text{en}}(T) \xrightarrow{\text{high } T} -k_B T \vartheta(0), \quad (\text{A.1a})$$

$$S_{\text{hyb}}^{\text{en}}(T) \xrightarrow{\text{high } T} k_B \vartheta(0) + k_B T \frac{\partial \vartheta(0)}{\partial T}, \quad (\text{A.1b})$$

$$U_{\text{hyb}}^{\text{en}}(T) \xrightarrow{\text{high } T} k_B T^2 \frac{\partial \vartheta(0)}{\partial T}. \quad (\text{A.1c})$$

It is worth re-emphasizing that $\vartheta(\varpi)$ depends in general on temperature T . This dependence is originated from the underlying response function, $\chi_{\text{SB}}(t)$ of Eq. (3.1).

Turn to the fermionic case that does not have the nonentanglement component; see Eq. (3.16). We would have rather

$$0 = A_{\text{hyb}}(\infty) = S_{\text{hyb}}(\infty) = U_{\text{hyb}}(\infty). \quad (\text{A.2})$$

These differ dramatically from the bosonic counterparts in Eq. (A.1). The detailed derivations are as follows.

To proceed, we consider Eq. (3.20) for the fermionic case, where $\varpi_n = (2n - 1)\pi/\beta$, a suitable high-

temperature approximant. Let us start with

$$A_{\text{hyb}}(T) = \frac{2}{\beta} \sum_{n=1}^{\infty} \vartheta(\varpi_n) \approx \frac{\kappa}{\beta} \vartheta(\varpi_1), \quad (\text{A.3})$$

This is the lowest Matsubara frequency based scheme, with $\varpi_1 = \pi/\beta$. The resultant $\kappa = \pi^2/4$ will be identified later, following the justifications, Eqs. (A.11)–(A.15) and comments there. To the end of this appendix, we will further propose an optimal resum scheme; see Eqs. (A.17)–(A.19).

Consider the temperature derivative on Eq. (A.3), which results in

$$S_{\text{hyb}}(T) \approx -\kappa k_B \vartheta(\varpi_1) - \frac{\kappa}{\beta} \pi k_B \vartheta'(\varpi_1) + \frac{\kappa}{T} \frac{\partial \vartheta(\varpi_1)}{\partial \beta}. \quad (\text{A.4})$$

The last term arises from the intrinsic temperature dependence of $\vartheta(\varpi)$, which is originated from the underlying Green's function, $G_{\text{SB}}(t)$ of Eq. (3.8). More precisely, $\partial \vartheta(\varpi)/\partial \beta \neq 0$, whenever there is *anharmonicity*. Note also that $\vartheta'(\varpi) \equiv \partial \vartheta/\partial \varpi$. Equation (A.4) amounts to

$$S_{\text{hyb}}(T) \approx -\kappa k_B \vartheta(\varpi_1) + U_{\text{hyb}}(T)/T. \quad (\text{A.5})$$

The first term is just $-A_{\text{hyb}}(T)/T$, with Eq. (A.3).

Let us express the hybridization free-energy and internal energy in terms of (noting that $\varpi_1 = \pi/\beta$)

$$A_{\text{hyb}}(T) \approx \frac{\kappa}{\pi} \varpi_1 \vartheta(\varpi_1), \quad (\text{A.6a})$$

$$U_{\text{hyb}}(T) \approx -\frac{\kappa}{\pi} \varpi_1^2 \vartheta'(\varpi_1) + \kappa \frac{\partial \vartheta(\varpi_1)}{\partial \beta}. \quad (\text{A.6b})$$

The high-temperature limit is then concerned with the three quantities, $\varpi \vartheta(\varpi)$, $\varpi^2 \vartheta'(\varpi)$ and $\partial \vartheta(\varpi)/\partial \beta$, in the $\varpi \rightarrow \infty$ regime. The first two via Eq. (3.22) are

$$\begin{aligned} \varpi \vartheta(\varpi) &= \text{Im} \int_0^1 \frac{d\lambda}{\lambda} \varpi \tilde{G}_{\text{SB}}(i\varpi; \lambda), \\ \varpi^2 \vartheta'(\varpi) &= \text{Im} \int_0^1 \frac{d\lambda}{\lambda} \varpi^2 \frac{\partial}{\partial \varpi} \tilde{G}_{\text{SB}}(i\varpi; \lambda). \end{aligned} \quad (\text{A.7})$$

By using the asymptotics of $\varpi e^{-\varpi t} \rightarrow 2\delta(t)$, we have

$$\varpi \tilde{G}_{\text{SB}}(i\varpi) = \varpi \int_0^{\infty} dt e^{-\varpi t} G_{\text{SB}}(t) \xrightarrow{\varpi \rightarrow \infty} G_{\text{SB}}(t=0).$$

Moreover, by using $\varpi^2 e^{-\varpi t} \rightarrow -2\dot{\delta}(t)$, we have

$$\begin{aligned} \varpi^2 \frac{d}{d\varpi} \tilde{G}_{\text{SB}}(i\varpi) &= - \int_0^{\infty} dt (\varpi^2 e^{-\varpi t}) [t G_{\text{SB}}(t)] \\ &\xrightarrow{\varpi \rightarrow \infty} 2 \int_0^{\infty} dt \dot{\delta}(t) [t G_{\text{SB}}(t)] \\ &= -G_{\text{SB}}(t=0). \end{aligned}$$

We can therefore write the limiting values of Eq. (A.7) as

$$\lim_{T \rightarrow \infty} \varpi \vartheta(\varpi) = - \lim_{T \rightarrow \infty} \varpi^2 \vartheta'(\varpi), \quad (\text{A.8})$$

with

$$\lim_{T \rightarrow \infty} \varpi \vartheta(\varpi) = \text{Im} \int_0^1 \frac{d\lambda}{\lambda} G_{\text{SB}}(t=0; \lambda) = 0. \quad (\text{A.9})$$

The last identity follows Eq. (3.12). Moreover, for fermionic hybrid systems in the high-temperature limit, the intrinsic temperature-dependence of $\vartheta(\varpi)$ via the Green's function would be saturated. In other words,

$$\lim_{\beta \rightarrow 0} \frac{\partial \vartheta(\varpi)}{\partial \beta} = 0. \quad (\text{A.10})$$

By applying Eqs. (A.8)–(A.10) for the $T \rightarrow \infty$ limiting values of Eq. (A.6), we obtain immediately all identities in Eq. (A.2).

We are now in the position to elaborate the parameter, $\kappa = \pi^2/4$, exploited in the second identity of Eq. (A.3). Let us revisit this identity, with the parameter κ the formal expression,

$$\kappa = \frac{2}{\vartheta(\varpi_1)} \sum_{n=1}^{\infty} \vartheta(\varpi_n). \quad (\text{A.11})$$

The involving $\{\varpi_n\}$ are the Matsubara frequencies, arising from the Fermi function expansion,

$$\frac{1}{1 + e^{\beta\omega}} = \frac{1}{2} - 2 \sum_{n=1}^{\infty} \frac{\omega/\beta}{\omega^2 + \varpi_n^2}. \quad (\text{A.12})$$

Consider then the high-temperature approximation,

$$\frac{\omega/\beta}{\omega^2 + \varpi_n^2} \approx \frac{\beta\omega}{(2n-1)^2 \pi^2} + \mathcal{O}[(\beta\omega)^3]. \quad (\text{A.13})$$

Therefore,

$$\sum_{n=1}^{\infty} \frac{\omega/\beta}{\omega^2 + \varpi_n^2} \approx \frac{\beta\omega}{\pi^2} \sum_{n=1}^{\infty} \frac{1}{(2n-1)^2} = \frac{\beta\omega}{\pi^2} \frac{\pi^2}{8}. \quad (\text{A.14})$$

Together with $\frac{\omega/\beta}{\omega^2 + \varpi_1^2} \approx \frac{\beta\omega}{\pi^2}$ via Eq. (A.13), we obtain

$$\sum_{n=1}^{\infty} \frac{\omega/\beta}{\omega^2 + \varpi_n^2} \approx \frac{\pi^2}{8} \frac{\omega/\beta}{\omega^2 + \varpi_1^2}. \quad (\text{A.15})$$

The factor of $\pi^2/8$ represents the ratio between the linear-order expansion and the lowest Matsubara frequency expansion. Remarkable, whenever the high-temperature asymptotic behaviors are concerned with, this ratio is generic and transferable to such as Eq. (A.11), where $\kappa = 2\pi^2/8 = \pi^2/4$. This is the value of κ in Eqs. (A.3)–(A.6).

For a close comparison with an optimized scheme [cf. Eq. (A.17)], we summarize the above high-temperature approximant, in terms of the Fermi function, Eq. (A.12). That is

$$\frac{1}{1 + e^{\beta\omega}} \approx \frac{1}{2} - \frac{\pi^2}{4} \frac{\omega/\beta}{\omega^2 + (\pi/\beta)^2} + \mathcal{O}[(\beta\omega)^3]. \quad (\text{A.16})$$

The value of $\varpi_1 = \pi/\beta$ is substituted explicitly.

On the other hand, it is well-known the best sum-over-poles expansion for Bose or Fermi functions is the Padé spectrum decomposition scheme.^{63–65} For the high-temperature asymptotics, it requires only the lowest-order Padé [0/1] approximant that reads

$$\frac{1}{1 + e^{\beta\omega}} \approx \frac{1}{2} - \frac{3\omega/\beta}{\omega^2 + (\sqrt{12}/\beta)^2} + \mathcal{O}[(\beta\omega)^5]. \quad (\text{A.17})$$

Its advantage over Eq.(A.16) is clearly evident. The involved single pole-related frequency is no longer $\varpi_1 = \pi/\beta$, but rather $\varpi_a \equiv \sqrt{12}/\beta$. The associated param-

eter is now $\kappa_a = 3$. More important, Eq.(A.17) suggests Eq.(A.6) be modified with

$$A_{\text{hyb}}(T) \approx \frac{\kappa_a}{\xi_a} \varpi_a \vartheta(\varpi_a), \quad (\text{A.18a})$$

$$U_{\text{hyb}}(T) \approx -\frac{\kappa_a}{\xi_a} \varpi_a^2 \vartheta'(\varpi_a) + \kappa_a \frac{\partial \vartheta(\varpi_a)}{\partial \beta}, \quad (\text{A.18b})$$

where

$$\kappa_a = 3, \quad \xi_a = \sqrt{12} \quad \text{and} \quad \varpi_a = \xi_a/\beta. \quad (\text{A.19})$$

-
- * Authors of equal contributions
† Electronic address: yanyj@ustc.edu.cn
- ¹ Y. Dubi and M. Di Ventra, *Rev. Mod. Phys.* **83**, 131 (2011).
 - ² J. P. Pekola, *Nat. Phys.* **11**, 118 (2015).
 - ³ J. Millen and A. Xuereb, *New J. Phys.* **18**, 011002 (2016).
 - ⁴ E. Geva and R. Kosloff, *J. Chem. Phys.* **104**, 7681 (1996).
 - ⁵ M. Horodecki and J. Oppenheim, *Nat. Commun.* **4**, 2059 (2013).
 - ⁶ P. Skrzypczyk, A. J. Short, and S. Popescu, *Nat. Commun.* **5**, 4185 (2014).
 - ⁷ N. Freitas and J. Pablo Paz, *Phys. Rev. E* **95**, 012146 (2017).
 - ⁸ Z. Merali, *Nat. News* **551**, 20 (2017).
 - ⁹ *Thermodynamics in the Quantum Regime: Fundamental Aspects and New Directions*, edited by F. Binder, L. A. Correa, C. Gogolin, J. Anders, and G. Adesso, Springer Nature Switzerland AG, 2018, *Fundamental Theories of Physics* 195.
 - ¹⁰ A. Einstein, in *Autobiographical Notes*, edited by P. A. Schilpp, Open Court Publishing, La Salle, 1979.
 - ¹¹ H. Kleinert, *Path Integrals in Quantum Mechanics, Statistics, Polymer Physics, and Financial Markets*, World Scientific, Singapore, 5th edition, 2009.
 - ¹² U. Weiss, *Quantum Dissipative Systems*, World Scientific, Singapore, 2012, 4rd ed.
 - ¹³ Y. J. Yan and R. X. Xu, *Annu. Rev. Phys. Chem.* **56**, 187 (2005).
 - ¹⁴ R. P. Feynman and F. L. Vernon, Jr., *Ann. Phys.* **24**, 118 (1963).
 - ¹⁵ S. Weiss, J. Eckel, M. Thorwart, and R. Egger, *Phys. Rev. B* **77**, 195316 (2008).
 - ¹⁶ L. Mühlbacher and E. Rabani, *Phys. Rev. Lett.* **100**, 176403 (2008).
 - ¹⁷ Y. Tanimura and R. Kubo, *J. Phys. Soc. Jpn.* **58**, 101 (1989).
 - ¹⁸ Y. Tanimura, *Phys. Rev. A* **41**, 6676 (1990).
 - ¹⁹ R. X. Xu, P. Cui, X. Q. Li, Y. Mo, and Y. J. Yan, *J. Chem. Phys.* **122**, 041103 (2005).
 - ²⁰ R. X. Xu and Y. J. Yan, *Phys. Rev. E* **75**, 031107 (2007).
 - ²¹ J. S. Jin, X. Zheng, and Y. J. Yan, *J. Chem. Phys.* **128**, 234703 (2008).
 - ²² Y. Tanimura, *J. Phys. Soc. Jpn.* **75**, 082001 (2006).
 - ²³ Y. Tanimura, *J. Chem. Phys.* **153**, 020901 (2020).
 - ²⁴ J. J. Ding, J. Xu, J. Hu, R. X. Xu, and Y. J. Yan, *J. Chem. Phys.* **135**, 164107 (2011).
 - ²⁵ J. J. Ding, R. X. Xu, and Y. J. Yan, *J. Chem. Phys.* **136**, 224103 (2012).
 - ²⁶ Z. H. Li, N. H. Tong, X. Zheng, D. Hou, J. H. Wei, J. Hu, and Y. J. Yan, *Phys. Rev. Lett.* **109**, 266403 (2012).
 - ²⁷ X. Zheng, R. X. Xu, J. Xu, J. S. Jin, J. Hu, and Y. J. Yan, *Prog. Chem.* **24**, 1129 (2012), <https://www.researchgate.net/publication/281547241>.
 - ²⁸ X. Zheng, Y. J. Yan, and M. Di Ventra, *Phys. Rev. Lett.* **111**, 086601 (2013).
 - ²⁹ L. Z. Ye, X. L. Wang, D. Hou, R. X. Xu, X. Zheng, and Y. J. Yan, *WIREs Comp. Mol. Sci.* **6**, 608 (2016).
 - ³⁰ Y. J. Yan, *J. Chem. Phys.* **140**, 054105 (2014).
 - ³¹ Y. J. Yan, J. S. Jin, R. X. Xu, and X. Zheng, *Frontiers in Physics* **11**, 110306 (2016).
 - ³² H. D. Zhang, R. X. Xu, X. Zheng, and Y. J. Yan, *Mol. Phys.* **116**, 780 (2018), Special Issue, “Molecular Physics in China”.
 - ³³ Y. Wang, R. X. Xu, and Y. J. Yan, *J. Chem. Phys.* **152**, 041102 (2020).
 - ³⁴ J. S. Jin, S. K. Wang, X. Zheng, and Y. J. Yan, *J. Chem. Phys.* **142**, 234108 (2015).
 - ³⁵ J. S. Jin, *Phys. Rev. B* **101**, 235144 (2020).
 - ³⁶ P. L. Du, Y. Wang, R. X. Xu, H. D. Zhang, and Y. J. Yan, *J. Chem. Phys.* **152**, 034102 (2020).
 - ³⁷ K. Funo and H. T. Quan, *Phys. Rev. Lett.* **121**, 040602 (2018).
 - ³⁸ Y. Tanimura, *J. Chem. Phys.* **141**, 044114 (2014).
 - ³⁹ Y. Tanimura, *J. Chem. Phys.* **142**, 144110 (2015).
 - ⁴⁰ A. Kato and Y. Tanimura, in *Thermodynamics in the Quantum Regime: Fundamental Aspects and New Directions*, edited by F. Binder, L. A. Correa, C. Gogolin, J. Anders, and G. Adesso, pages 579–595, Springer Nature Switzerland AG, 2018, *Fundamental Theories of Physics* 195.
 - ⁴¹ J. G. Kirkwood, *J. Chem. Phys.* **3**, 300 (1935).
 - ⁴² R. C. Shuela and E. R. Muller, *Phys. Stat. Sol. (b)* **43**, 413 (1971).
 - ⁴³ R. van Zon, L. Hernández de la Peña, G. H. Peslherbe, and J. Schofield, *Phys. Rev. E* **78**, 041103 (2008).
 - ⁴⁴ R. van Zon, L. Hernández de la Peña, G. H. Peslherbe, and J. Schofield, *Phys. Rev. E* **78**, 041104 (2008).
 - ⁴⁵ J. E. Hirsch and R. M. Fye, *Phys. Rev. Lett.* **56**, 2521 (1986).
 - ⁴⁶ E. Gull, A. J. Millis, A. I. Lichtenstein, A. N. Rubtsov,

- M. Troyer, and P. Werner, Rev. Mod. Phys. **83**, 349 (2011).
- ⁴⁷ S. R. White, Phys. Rev. Lett. **69**, 2863 (1992).
- ⁴⁸ G. Vidal, Phys. Rev. Lett. **91**, 147902 (2003).
- ⁴⁹ K. G. Wilson, Rev. Mod. Phys. **47**, 773 (1975).
- ⁵⁰ R. Bulla, T. A. Costi, and T. Pruschke, Rev. Mod. Phys. **80**, 395 (2008).
- ⁵¹ L. P. Kadanoff and G. Baym, *Quantum Statistical Mechanics*, Benjamin, New York, 1962.
- ⁵² H. D. Meyer, U. Manthe, and L. Cederbaum, Chem. Phys. Lett. **165**, 73 (1990).
- ⁵³ H. B. Wang and M. Thoss, J. Chem. Phys. **119**, 1289 (2003).
- ⁵⁴ H. Gong, Y. Wang, H. D. Zhang, Q. Qiao, R. X. Xu, X. Zheng, and Y. J. Yan, J. Chem. Phys. (2020), <http://arxiv.org/abs/2008.04087>.
- ⁵⁵ R. H. Foote, D. R. Ward, J. R. Prance, J. K. Gamble, E. Nielsen, B. Thorgrimsson, D. E. Savage, A. L. Saraiva, M. Friesen, S. N. Coppersmith, and M. A. Eriksson, Appl. Phys. Lett. **107**, 103112 (2015).
- ⁵⁶ M. Veldhorst, C. H. Yang, J. C. C. Hwang, W. Huang, J. P. Dehollain, J. T. Muhonen, S. Simmons, A. Laucht, F. E. Hudson, K. M. Itoh, A. Morello, and A. S. Dzurak, Nature **526**, 410 (2015).
- ⁵⁷ J. M. Gambetta, A. A. Houck, and A. Blais, Phys. Rev. Lett. **106**, 030502 (2011).
- ⁵⁸ X. Gu, A. F. Kockum, Y. X. Liu, and F. Nori, Phys. Rep. **718-719**, 1 (2017).
- ⁵⁹ P. Scarlino, D. J. van Woerkom, U. Mendes, J. Koski, A. J. Landig, C. K. Andersen, S. Gasparinetti, C. Reichl, W. Wegscheider, K. Ensslin, T. Ihn, A. Blais, and A. Wallraff, Nature Comm. **10**, 3011 (2019).
- ⁶⁰ D. Kafri, C. Quintana, Y. Chen, A. Shabani, J. M. Martinis, and H. Neven, Phys. Rev. A **95**, 52333 (2017).
- ⁶¹ A. Damascelli, Z. Hussain, and Z. X. Shen, Rev. Mod. Phys. **75**, 473 (2003).
- ⁶² O. Y. Kolesnychenko, G. M. M. Heijnen, A. K. Zhuravlev, R. de Kort, M. I. Katsnelson, A. I. Lichtenstein, and H. van Kempen, Phys. Rev. B **72**, 085456 (2005).
- ⁶³ T. Ozaki, Phys. Rev. B **75**, 035123 (2007).
- ⁶⁴ J. Hu, R. X. Xu, and Y. J. Yan, J. Chem. Phys. **133**, 101106 (2010).
- ⁶⁵ J. Hu, M. Luo, F. Jiang, R. X. Xu, and Y. J. Yan, J. Chem. Phys. **134**, 244106 (2011).